Chapter

Electric Field-Induced Magnetization Reversal of Multiferroic Nanomagnet

Jiahao Liu and Liang Fang

Abstract

Using the inverse piezoelectric effect and inverse magnetostrictive effect in a multiferroic heterojunction, an electric field is able to control the magnetization switching of a uniaxial nanomagnet. Compared with traditional spintronic devices based on magnetic field, multiferroic nanomagnet devices have the advantages of ultra-low consumption and high radiation resistance, showing great application potential in modern high-integrated circuits and military electronic systems. However, the difficulties of electric field control of complete magnetization reversal of the nanomagnet and nanomagnet arrays in a nanomagnetic logic gate still restrict the developments of multiferroic nanomagnet device. In this chapter, the uniaxial nanomagnets in multiferroic heterojunctions are mainly discussed. The two core problems of the electric field control of nanomagnets and nanomagnetic logic gate are well solved.

Keywords: multiferroics, magnetization switching, spintronics, nanomagnet, straintronics

1. Introduction

Using the inverse piezoelectric effect and inverse magnetostrictive effect in a multiferroic heterojunction, an electric field is able to control the magnetization switching of a uniaxial nanomagnet. **Figure 1** is a multiferroic heterojunction structure, that is, a two-layer magnetoelectric composite structural system, which is formed by magnetoelastic coupling of a magnetostrictive layer and a piezoelectric layer. The electric field-controlled nanomagnet in a multiferroic heterojunction essentially uses multi-field coupling of "electric-stress-magnetic." Applying a small voltage to the piezoelectric layer, the piezoelectric layer will produce uniaxial strain, which is transformed into a stress applying on the magnetostrictive layer by magnetoelastic coupling, causing the magnetization direction of the magnetostrictive layer to rotate perpendicular to the stress. If the magnetostrictive layer is constructed as a uniaxially shaped nanomagnet, the strain will reverse the magnetization direction of the nanomagnet to a logically "NULL" state, pointing to the hard magnetization axis, which is, the short axis direction. At this time, if the voltage is released (stress revocation), the nanomagnet will flip to a certain stable logic state (original logic state or opposite logic state). This magnetic logic device based on the regulation mode of the multiferroic heterojunction magnetoelectric effect is called

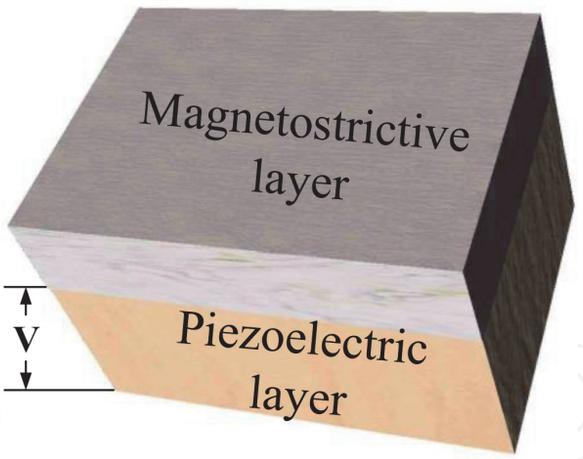

Figure 1.
Multiferroic heterojunction structure.

a multiferroic nanomagnet device. Multiferroic nanomagnet device is one of the most competitive spintronic devices due to its low energy consumption and high thermal stability [1]. It represents Boolean logic "0" and "1" in the magnetization directions along the long axis of a uniaxial nanomagnet [2] and can be corresponding to different states in the magnetic tunnel junction [3].

2. Voltage pulse-induced magnetization switching

The key to using the stress generated by the electric field to control the magnetization switching of the multiferroic nanomagnet is that the stress anisotropy must be larger than the shape anisotropy of the nanomagnet. An effective method to reduce the required stress anisotropy is to break the symmetry of the shape of the nanomagnet by slightly tilting the long axis of the nanomagnet to the direction of stress application. However, the effect of the tilt angle on the magnetization reversal of the nanomagnet is still inconclusive.

2.1 Model

Figure 2 presents the voltage-controlled multiferroic heterostructure. The red arrow indicates the direction of magnetization. The polar angle (out-of-plane) and the azimuth angle (in-plane) of the magnetization are θ and φ, respectively. Note that the magnet is at an angle to the direction of the electrodes.

The magnetization dynamic of a single elliptical nanomagnet meets the Landau-Lifshitz-Gilbert Eq. (5):

$$\frac{\mathrm{d}\vec{M}}{\mathrm{d}t} = -\gamma\vec{M} \times \overrightarrow{H_{eff}} - \frac{\alpha\gamma}{M_s}\left[\vec{M} \times \left(\vec{M} \times \overrightarrow{H_{eff}}\right)\right] \tag{1}$$

where α is the damping coefficient, $\overrightarrow{M}$ is the magnetic moment vector of the nanomagnet, M_s is the saturation magnetization, γ is the return ratio, and [5]:

$$\overrightarrow{H_{eff}} = -\frac{1}{\mu_0 V}\frac{\mathrm{d}E}{\mathrm{d}\vec{M}} \tag{2}$$

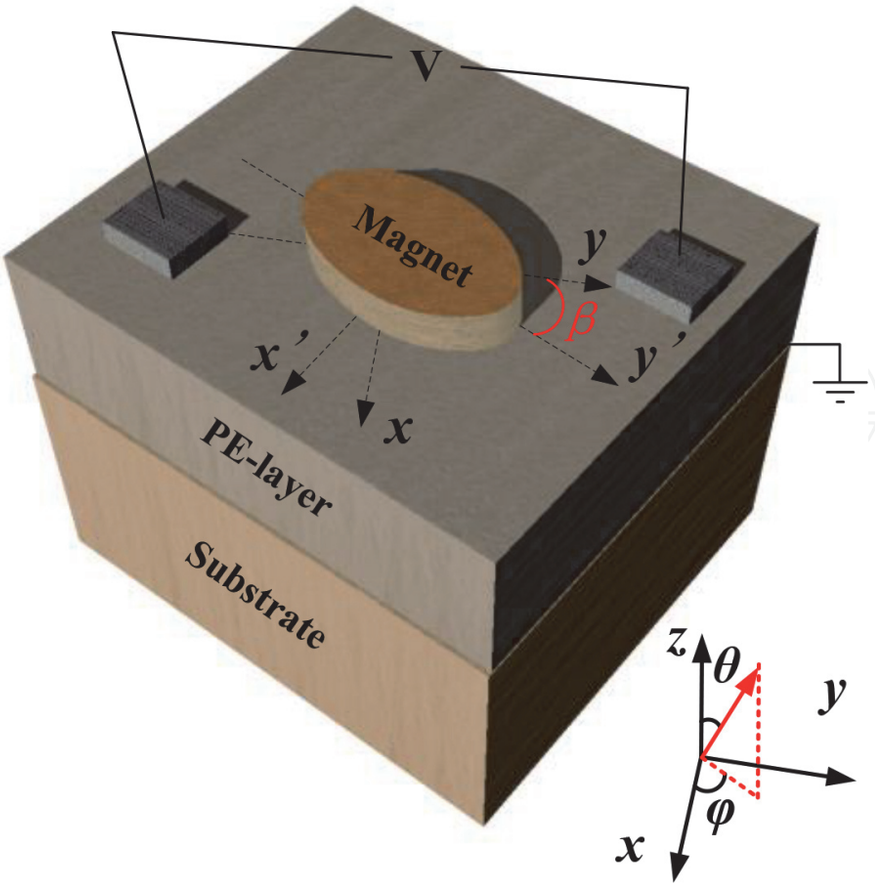

Figure 2.
Stress-regulated multiferroic tilted nanomagnet device [4].

is the effective field generated by a variety of energies (shape anisotropy energy, stress anisotropy energy, Zeeman energy, and thermal fluctuations), where $\mu_0 = 4\pi \times 10^{-7}$ is the vacuum permeability and V is the volume of each element. The stress is applied at the y direction, and the total energy E_{total} is the sum of demagnetization energy, exchange energy, shape anisotropy energy, stress anisotropy energy, and energy dissipation:

$$E_{\text{total}} = E_{\text{demagnetization}} + E_{\text{exchange}} + E_{\text{shape-anisotropy}} + E_{\text{stress-anisotropy}} + E_{\text{dissipation}} \tag{3}$$

For Terfenol-D as the magnetic material, the crystal anisotropy energy of is small, and thus is ignored in the calculation of the total energy. The exchange energy can also be neglected in the single domain particles of 100 nm × 50 nm × 20 nm [6]. The shape anisotropy energy of the nanomagnet can be written as [7]:

$$E_{\text{shape-anisotropy}} = \int -(\mu_0/2)\, \vec{\boldsymbol{M}} \cdot \vec{\boldsymbol{H}}_M \, \mathrm{d}V \tag{4}$$

where $\vec{\boldsymbol{M}}$ is the magnetic moment vector of the nanomagnet and $\vec{\boldsymbol{H}}_M$ is the shape anisotropy energy field, which can be expressed as [7]:

$$\vec{\boldsymbol{H}}_M = -N_{dx} M_x \hat{i} - N_{dy} M_y \hat{j} - N_{dz} M_z \hat{k} \tag{5}$$

$$E_{\text{shape}-\text{anisotropy}} = -(\mu_0/2)\left(M_s^2 V\right)\left[N_{dx}\cos^2\theta\sin^2\varphi + N_{dy}\sin^2\theta\sin^2\varphi + N_{dz}\cos^2\varphi\right] \tag{6}$$

where N_d is the demagnetization factor. For elliptical shaped nanomagnets, the demagnetization factors N_{dx}, N_{dy}, and N_{dz} can be calculated through [7]:

$$N_{dx} = \frac{\pi}{4}\left(\frac{th}{a}\right)\left[1 + \frac{5}{4}\left(\frac{a-b}{a}\right) + \frac{21}{16}\left(\frac{a-b}{a}\right)^2\right] \tag{7}$$

$$N_{dy} = \frac{\pi}{4}\left(\frac{th}{a}\right)\left[1 - \frac{1}{4}\left(\frac{a-b}{a}\right) - \frac{3}{16}\left(\frac{a-b}{a}\right)^2\right] \tag{8}$$

$$\mathrm{N_{dz}} = 1 - \mathrm{N_{dx}} - \mathrm{N_{dy}} \tag{9}$$

where a is the length of the long axis, b is the length of the short axis, and th is the thickness of the nanomagnet. For a nanomagnet whose tilt angle is β, as shown in **Figure 2**, the short axis and long axis of the nanomagnet rotate clockwise from the x axis and y axis to the x' axis and y' axis, respectively, and z' axis (not shown) is still at vertical direction. The shape anisotropy field components in the new coordinate system are:

$$h'_{\text{shape}-\text{anisotropy\_xx}} = -M_s N_{dx}\cos(\varphi+\beta)\sin\theta \tag{10}$$

$$h'_{\text{shape}-\text{anisotropy\_yy}} = -M_s N_{dy}\sin(\varphi+\beta)\sin\theta \tag{11}$$

$$h'_{\text{shape}-\text{anisotropy\_zz}} = -M_s N_{dz}\cos\theta \tag{12}$$

By the coordinate rotation conversion of (10)–(12), the field components of shape anisotropy of the tilted nanomagnet on the original coordinate axes become:

$$h_{\text{shape}-\text{anisotropy\_xx}} = -M_s\left(N_{dx}\cos(\varphi+\beta)\cos\beta + N_{dy}\sin(\varphi+\beta)\sin\beta\right)\sin\theta \tag{13}$$

$$h_{\text{shape}-\text{anisotropy\_yy}} = -M_s\left(-N_{dx}\cos(\varphi+\beta)\sin\beta + N_{dy}\sin(\varphi+\beta)\cos\beta\right)\sin\theta \tag{14}$$

$$h_{\text{shape}-\text{anisotropy\_zz}} = -M_s N_{dz}\cos\theta \tag{15}$$

The stress anisotropy energy of the nanomagnet is given by [7]:

$$E_{\text{stress}-\text{anisotropy}} = -\frac{3}{2}\lambda_s\sigma V\sin^2\theta\sin^2\varphi \tag{16}$$

where $3\lambda_s/2$ is the saturation magnetostriction and the stress σ is considered negative for compression and positive for tension. The stress is applied in the y direction, so there is only a field component in the y axis direction [8]:

$$h_{\text{stress}-\text{anisotropy\_yy}} = (3\lambda_s/M_s\mu_0)\sigma\sin\theta\sin\varphi \tag{17}$$

Considering the thermal fluctuations, the effect of random thermal fluctuations can be described by a random thermal field [9]:

$$h(t) = \sqrt{\frac{2\alpha kTf}{\gamma\mu_0 M_s V}}G_{(0,1)}(t) \tag{18}$$

where $k = 1.38 \times 10^{-23}$ J/K is the Boltzmann constant, $T = 300$ K is the room temperature, $f = 1$ GHz is the frequency of thermal noise oscillations, and $G_{(0,1)}$ represents a Gaussian function with a mean of 0 and a variance of 1. By combining the above functions, the effective field $\overrightarrow{\boldsymbol{H}_{eff}}$ can be obtained. A bias field can also be involved in the x direction if it is required. The components of each coordinate axis are:

$$h_x = -M_s\left(N_{dx}\cos(\varphi+\beta)\cos\beta + N_{dy}\cos(\varphi+\beta)\sin\beta\right)\sin\theta + \sqrt{\frac{2\alpha kTf}{\gamma\mu_0 M_s V}}\mathrm{G}_{(0,1)}(t) + h_{bias} \tag{19}$$

$$h_y = -M_s\left(N_{dx}\cos(\varphi+\beta)\sin\beta + N_{dy}\sin(\varphi+\beta)\cos\beta\right)\sin\theta + (3\lambda_s/M_s\mu_0)\sigma\sin\theta\sin\varphi + \sqrt{\frac{2\alpha kTf}{\gamma\mu_0 M_s V}}G_{(0,1)}(t) \tag{20}$$

$$h_z = -M_s N_{dz}\cos\theta + \sqrt{\frac{2\alpha kTf}{\gamma\mu_0 M_s V}}G_{(0,1)}(t) \tag{21}$$

2.2 Results and discussions

Biswas et al. used two pairs of electrodes to control the nanomagnet in the experiment to achieve a reliable 180° switching [10, 11]. However, since the two pairs of electrodes have to be operated in sequence, the nanomagnet needs a longer switching time. Fashami used a timed pulse to switch the nanomagnet by 180°, which is error-free and dissipates arbitrarily small energy [12]. However, in this scheme, a hard magnet is essential to break the energy symmetry, and a long switching time is required. Recently, a method of 180° switching has been proposed, in which a repeatable 180° nanomagnet switching was induced by voltage pulses. By setting suitable amplitude, width, and period of the voltage pulse, it is possible to achieve repeatable 180° switchings without a magnetic field [13, 14]. However, although this solution can achieve repeatable magnetic switching, the first switching requires a large start-up time, making the first switching time much longer [15, 16]. In magnetic storage and logic application, the first switching is most often needed. More importantly, these studies did not consider the thermal fluctuations, which play an important role in the switching of the nanomagnet. In conclusion, fast switching of nanomagnets at room temperature is still a challenge for straintronics in the application of logic storage and computing. This section introduces a fast switching method of nanomagnets at room temperature. The structure is shown in **Figure 1** of the previous section. The authors use OOMMF software to simulate and study the switching of nanomagnets.

The authors chose PMN-PT ($Pb(Mg_{1/3}Nb_{2/3})O_3$-$PbTiO_3$) as the piezoelectric layer material to use its higher piezoelectric coefficient [17, 18]. And for the magnetic material, the authors chose Terfenol-D ($Tb_{0.7}Dy_{0.3}Fe_2$), because the magnetocrystalline anisotropy can be smaller [19]. The parameters are shown in **Table 1**.

Since (Object Oriented Micromagnetic Framework) software [20] cannot directly set the stress anisotropy energy, the authors use the uniaxial anisotropy energy acting in the direction of $(-\cos\beta\ \sin\beta\ 0)$ for replace. Accordingly [6]:

$$K = -\frac{3}{2}\lambda_s\sigma V \tag{22}$$

Symbol	Quantity	Value
Y	young's modulus	8×10^{10} Pa
$3\lambda_s$ 2	saturated magnetostriction	6×10^{-4}
α	damping coefficient	0.1
K	magnetocrystalline anisotropy constant	0
M_s	saturated magnetization	8×10^{5} A m
a	length of long axis	100 nm
b	length of short axis	50 nm
th	thickness of magnetic layer	20 nm
t_p	thickness of piezoelectric layer	400 nm
υ	Poisson's ratio	0.3

Table 1.
Parameters of multiferroic heterostructure.

The size of nanomagnet is 51 nm × 102 nm × 21 nm. The selection of large aspect ratio and thickness can reduce C-shaped and eddy vortex errors [21]. The mesh size of OOMMF is 3 nm × 3 nm × 3 nm. Magnetization toward up and down is defined as logic "1" and "0," respectively. The initial state of the nanomagnet is assumed as logic "1."

Before studying voltage pulse-induced 180° switching, the first step is to ensure that the magnetization direction of the nanomagnet is able to rotate by more than 90° (below x axis). **Figure 3** shows that minimum stress is required for the nanomagnet to rotate by more than 90° when the stress is applied in different directions ($0 < \beta < 10°$) [22]. A small β can reduce the required stress, which makes it easier for the nanomagnet to rotate by more than 90°. However, as β increases, the required stress also increases. This is because the stress tends to make the magnetization direction perpendicular to the axis of the electrodes pair, i.e., to flip to the x' axis. When β is larger, the x' axis will also make a larger deflection angle with the x axis. This makes nanomagnet difficult to rotate by more than 90°. Even so, when $0 < \beta < 7°$, the required stress is less than the scheme with the electrodes' pair axis along the long axis of the nanomagnet ($\beta = 0$).

In the second step, optimal voltage pulse should be set to make the switching time as short as possible. The authors apply a stress of 100 MPa to the nanomagnet (voltage pulse peak of 225 mVs), which is sufficient for the nanomagnet to rotate by more than 90°. **Figure 4** shows the optimal waveform setting and dynamic

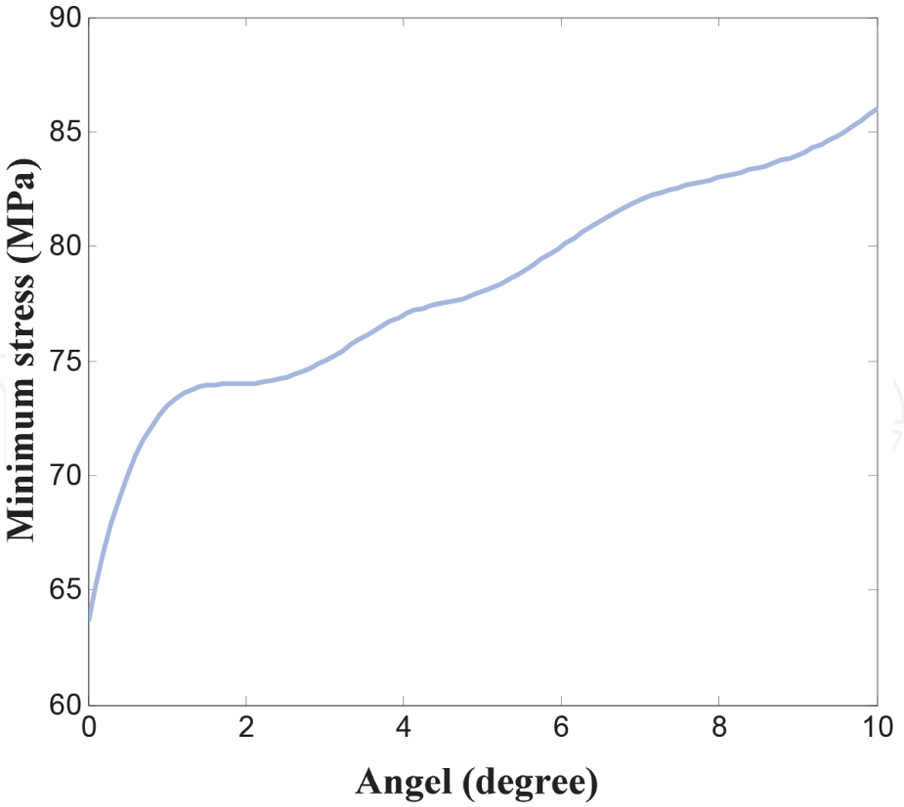

Figure 3.
Minimum stress required for the nanomagnet to rotate by more than 90° with different tilt angles β of electrodes' pair axis [22].

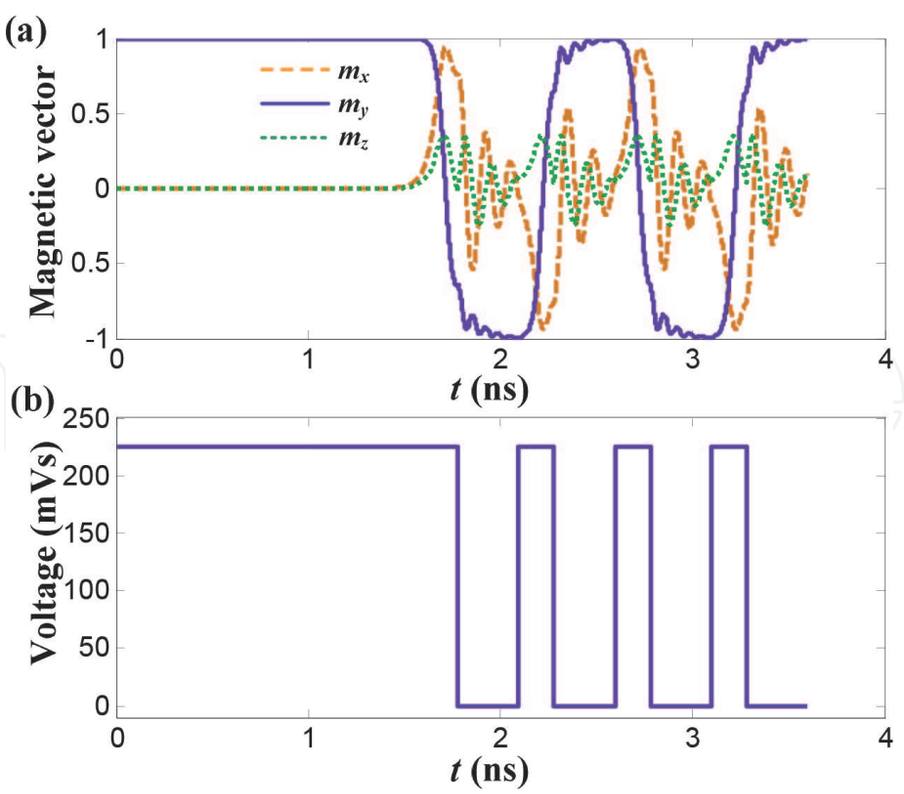

Figure 4.
180° switching with the stress electrodes' pair axis along the long axis of the nanomagnet. (a) Dynamic magnetization. (b) Voltage pulse waveform.

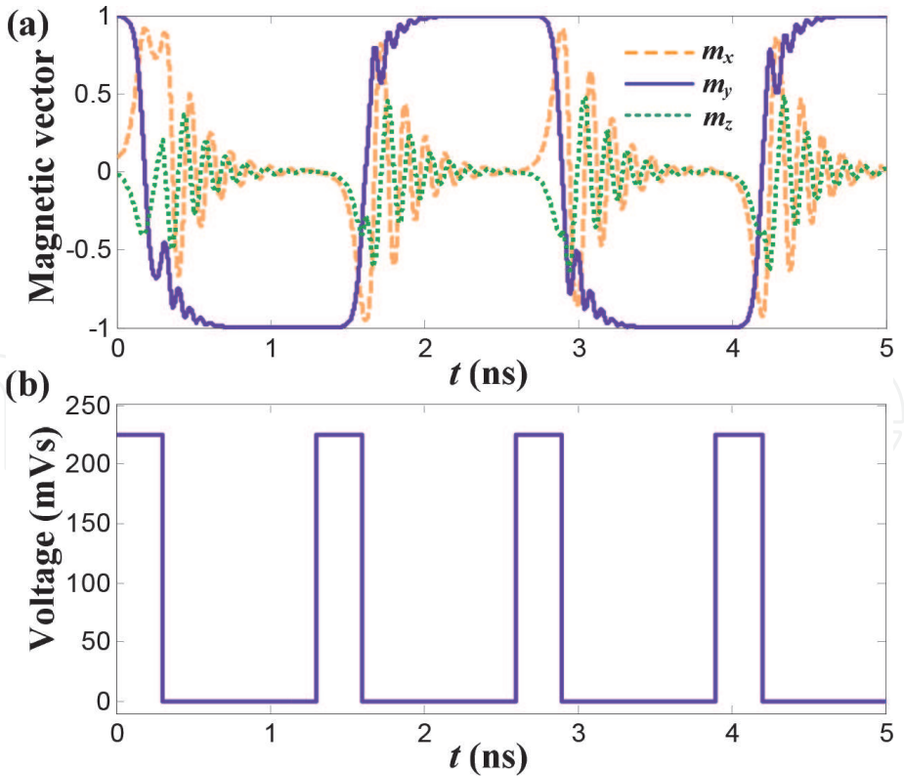

Figure 5.
Repeated 180° switching with β = 5° under room temperature. (a) Dynamic magnetization. (b) Voltage pulse waveform.

magnetization of the repeatable 180° switchings in the nanomagnet, when the electrodes' pair axis is aligned with the long axis of the nanomagnet ($\beta = 0$). **Figure 5(a)** is the dynamic magnetization of repeatable 180° switchings in the nanomagnet. It can be seen from the inset that the nanomagnet requires the voltage to be applied for a long period of time (1.6 ns) before it can enter the switching cycle. This is because the nanomagnet has equal probability of reaching either orientation when the stress is applying along the long axis. Therefore, the nanomagnet will enter a magnetization direction selection period before it can be flipped. This start-up time greatly increases the first switching time of the nanomagnet. **Figure 5(b)** shows the optimal voltage pulse waveform for the nanomagnet switching. The minimum start-up time of the nanomagnet $t_{\text{start-up}} = 1.600$ ns, the minimum voltage pulse width $t_{\text{width}} = 0.180$ ns, and the minimum pulse interval time $t_{\text{interval}} = 0.320$ ns. The minimum switching period of the nanomagnet is the sum of the minimum voltage pulse width and the minimum interval time, $T = t_{\text{width}} + t_{\text{interval}} = 0.500$ ns, and the maximum switching frequency $f = 1/T = 2.000$ GHz. The time that the nanomagnet completes the initial switching is the sum of the minimum start-up time and the minimum switching period: $t_{\text{initial}} = t_{\text{starting}} + T = 2.070$ ns.

If the electrodes' pair axis is not aligned with the long axis of the nanomagnet, but is tilted by a small angle β, the nanomagnet will have a tendency to select where to flip. For $\beta > 0$, nanomagnets tend to flip clockwise. This allows the nanomagnet to require no start-up time during the first switching, greatly increasing the efficiency of the initial switching.

Figure 6 shows the dynamic magnetization of the switchings and optimal voltage pulse waveform when $\beta = 5°$. The nanomagnet has no start-up time and directly enters the switching cycle. The minimum voltage pulse width $t_{\text{width}} = 0.162$ ns, and the minimum pulse interval time $t_{\text{interval}} = 0.312$ ns. Therefore, the minimum switching period of the nanomagnet is the sum of the minimum voltage pulse width

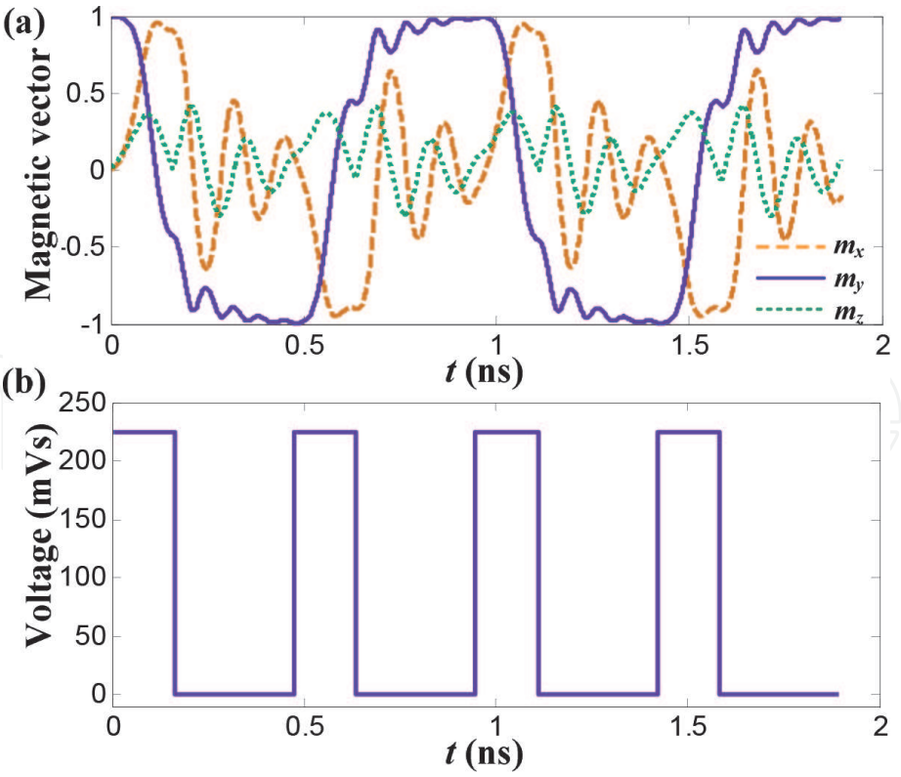

Figure 6.
Fast 180° switching with β = 5°. *(a) Dynamic magnetization. (b) Voltage pulse waveform.*

and the minimum interval time, $T = t_{\text{width}} + t_{\text{interval}} = 0.447$ ns, and the maximum switching frequency $f = 1/T = 2.110$ GHz. The time that the nanomagnet completes the initial switching is the same as the minimum switching cycle: $t_{\text{initial}} = T = 0.474$ ns. This is only about 1/5 of **Figure 4**.

The authors continue to calculate the minimum time and maximum switching frequency for the nanomagnet to complete the 180° switching. The voltage pulse peak is controlled to be a constant 225 mVs.

As shown in **Figure 7**, since there is no start-up time, the minimum initial switching time of the nanomagnet with $\beta > 0$ is significantly smaller than that of the nanomagnet with $\beta = 0$. The minimum pulse width decreases as β increases. For $\beta > 6°$, although the minimum pulse width continues to decrease as β increases, the minimum interval increases in the meanwhile. When $4° < \beta < 9°$, the minimum total initial switching time is small and the maximum switching frequency is also larger than that of **Figure 5** ($\beta = 0$). Based on the above factors, β should be chosen to be around 5°. So nanomagnets will have less required stress, larger switching frequency, and shorter initial switching time.

Although voltage pulse-induced magnetization switching is very energy efficient, the possibility of operating at room temperature remains to be discussed, which plays an important role in the switching. In this section, the switching of the nanomagnet at room temperature (300 K) is calculated. Since OOMMF software could be computationally expensive and time-consuming to simulate the switching at room temperature, the authors use the mathematical stress model to calculate the switching of the nanomagnet at room temperature.

Firstly, the authors apply a stress of 100 MPa to the electrodes and observe the dynamic magnetization of the nanomagnet. The magnetization rotates by more than 90° at 0.1844–0.3470 ns and is most close to logic "0" at 0.2574 ns, meaning that $t_{\text{width}} = 0.2574$ ns. If the stress is removed at 0.2574 ns, the nanomagnet will flip to logic "0" at 0.7427 ns, meaning that $t_{\text{interval}} = 0.8856$ ns. Obviously, at room temperature, both t_{width} and t_{interval} are much larger than that at 0 K.

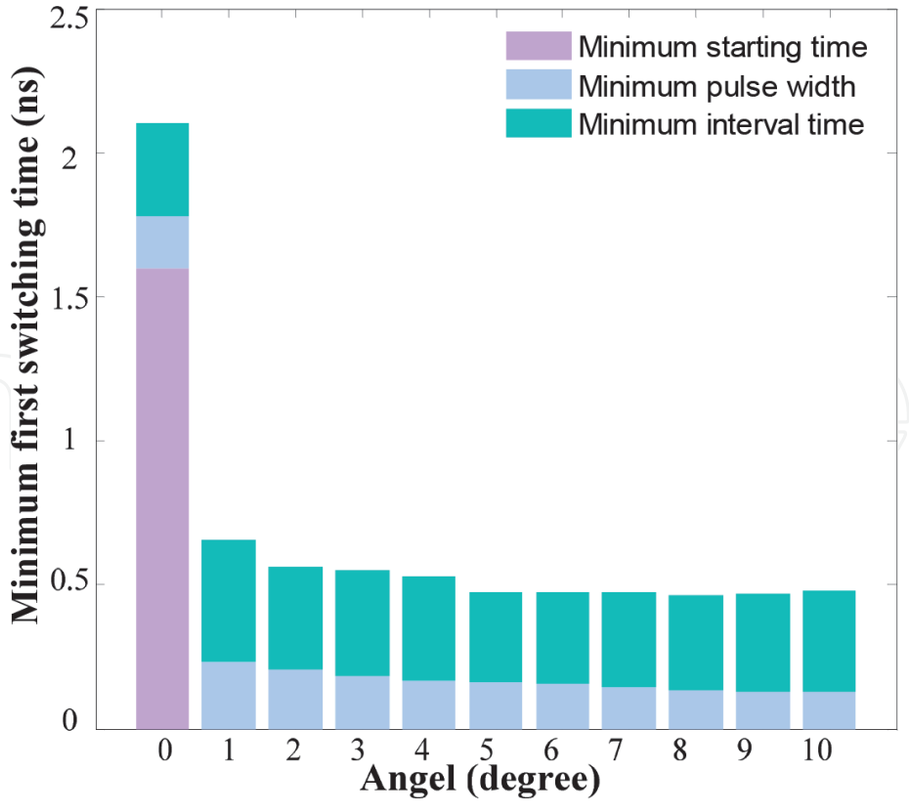

Figure 7.
Minimum switching times of the nanomagnet changes with the tilt angles of the electrode pair axis.

Secondly, the authors try to control the switching by voltage pulse of t_{width} = 0.2574 ns and $t_{interval}$ = 0.8856 ns at room temperature. Unfortunately, the nanomagnet succeeds to be switched to logic "0," but never return back to logic "1" again. Under the influence of thermal fluctuations, the nanomagnet needs to remain in a stable logic state for a longer period of time before it can be switched again.

Thirdly, t_{width} = 0.3 ns (it can be chosen from 0.1844 to 0.3470 ns) and $t_{interval}$ = 1 ns are given to gain repeated switchings. As shown in **Figure 5**, the nanomagnet converts back and forth between two logic states at room temperature successfully.

The switching cycle is 1.3 ns. One thing that must be pointed out is that the simulations assume the ideal voltage pulse waveform. The effects of the rising and falling edges of the actual voltage pulse are not considered. Besides, through the calculation of the model, $t_{interval}$ can be long enough but t_{width} can be only chosen from 0.1844 to 0.3470 ns. Actually, pulse width needed for 180° switching will not be a constant in the presence of thermal noise. The pulse width error of less than 0.2 ns will be a challenge under room temperature, which is the disadvantage of this scheme. These will need to be further studied in the subsequent experimental work.

Due to the symmetry, setting the initial logic as "0" or setting the electrodes' pair axis, a clockwise deflection will get the same result, which is not described in this paper for clarity.

2.3 Conclusion

The efficient 180° switching of the magnetization direction of the nanomagnet is the key to straintronic devices in the application of magnetic storage and logic. The voltage pulse-induced repeatable 180° switching is a fast and low energy consumption scheme, but the initial switching requires a large start-up time and thermal

fluctuation is a great challenge. This method overcomes the start-up time of the initial switching by rotating the stress electrodes' pair axis by a small angle from the long axis of the nanomagnet. Using OOMMF software for simulation, the optimal voltage pulse waveform to control the 180° switchings of the nanomagnet is calculated, and the influence of electrodes' pair axis tilt angle β is studied. The results show that when the tilt angle β is about 5°, the nanomagnet has lower switching frequency, shorter initial switching time, and less required stress. Repeated switching at room temperature is calculated by mathematical model. The switching time is longer under the influence of thermal fluctuations. These findings will provide possible guidance for straintronic devices in the application of magnetic storage and logic.

3. Electric control of nanomagnetic logic gate

The previous section introduced the electric field regulation of a single nanomagnet, and this section will continue to discuss the electric field control method for nanomagnet arrays. Information transmission and calculations in nanomagnetic logic rely on the control of nanomagnet array. The problem of efficient information transmission is well solved [6]. However, electric-controlled magnetic logic gate is still a major challenge. Imre et al. used five single-axis nanomagnets to build a majority logic gate [2], which made nanomagnetic logic possible. However, this logic gate requires multiple clock controls to ensure correct logic calculations. Gypens et al. used 19 dipole-coupled uniaxial nanomagnets to form a stable system and built a NAND (NOR) logic gate that can be accurately calculated [23]. However, this solution requires more nanomagnets, which increases the NML area. Roy uses a multi-iron material to propose an ultra-low-energy NAND (OR) logic gate based on a magnetic tunnel junction [24]. However, this logic gate design requires casting multiple layers of materials, which increases the difficulty of manufacturing. Niemier et al. put forward a long axis tilted nanomagnet structure by using an edge-slanted nanomagnet and designed dual-input AND/OR logic gates based on it. Most studies now use this type of edge-slanted nanomagnet to achieve long axis tilted nanomagnet structures. However, there are three defects in edge-slanted nanomagnets: (1) This type of nanomagnet requires a larger size, thus increasing the NML space and introducing clock errors of the C-shape and eddy current that easily occur in large-sized nanomagnets. (2) Complex calculations caused by the irregular shape are inevitable. (3) More importantly, the irregular shape of nanomagnet increases the requirements of fabrication process.

From the above perspective, a more effective and more reliable design of basic magnetic logic gates is required to be proposed. The design should address two key issues: (1) how to eliminate C-shaped and eddy current clock errors and (2) how to reduce the complexities of calculations and fabrication process.

3.1 Design and analysis

In the previous section, the long axis tilted nanomagnet is introduced. As shown in **Figure 8(a)**, the long axis and short axis of the nanomagnet rotate from the x axis and y axis to the x' axis and y' axis, respectively. If the tilt angle that long axis makes with the direction of the electrodes is β, the included angles between long axis and the clock will be a larger one ($90° + \beta$) and a smaller one ($90° - \beta$). When driven by no other energy, the nanomagnet will flip toward the smaller angle after the stress is released. This is because the nanomagnet has higher anisotropy along the clock than that along the long axis and will spontaneously flip to the shape anisotropy potential

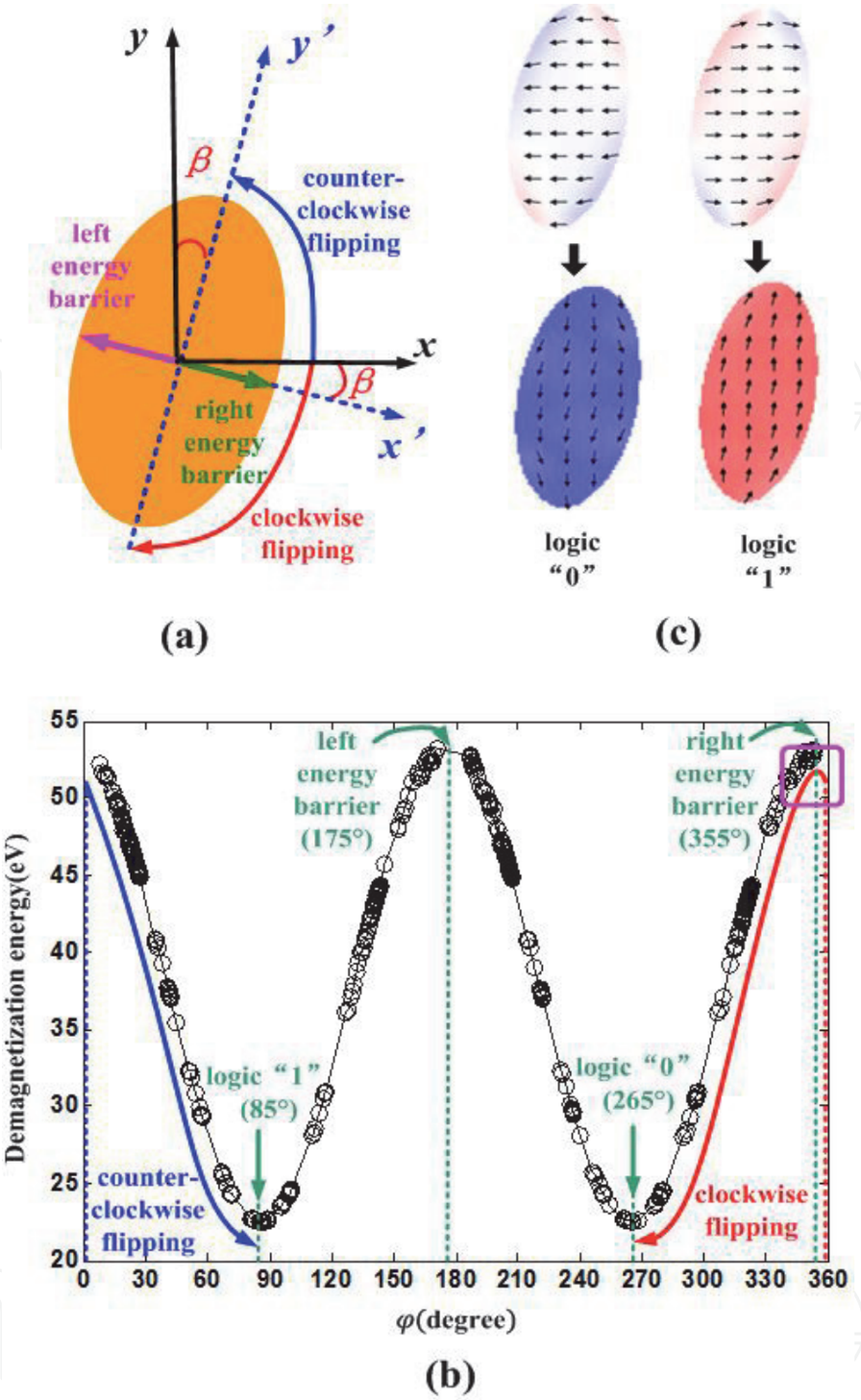

Figure 8.
(a) The nanomagnet is rotated clockwise by a small angle β. (b) the demagnetization energy is calculated as a function of φ. (c) the preferred magnetization is simulated by OOMMF.

well of the long axis. However, in the course of flipping toward the larger angle $(90° + \beta)$, it is necessary to cross the shape anisotropy barrier of the hard axis. As a consequence, the nanomagnet tends to flip toward the smaller angle $(90° - \beta)$ without the need of crossing the shape anisotropy barrier of the hard axis.

As shown in **Figure 8(b)**, for a nanomagnet with a tilt angle $\beta = 5°$, the demagnetization energy is calculated by OOMMF, as a function of φ. For the parameters, the authors have assumed a space size of 80 nm × 100 nm × 20 nm, mesh size of 2 nm × 2 nm × 2 nm, magnet dimensions of 50 nm × 100 nm × 20 nm, saturation magnetization of 800 kA/m, Gilbert damping constant of 0.5, and zero magnetocrystalline anisotropy. The high aspect ratio (2:1) and the small tilt angle

(β = 5°) of the nanomagnet are set to eliminate the C-shaped and eddy current clock errors. As shown in the inset, the demagnetization energy curve of the tilted nanomagnet is shifted 5° to the left, where logic "1" and "0" correspond to 85° and 265°, respectively, while "NULL" (high energy state) states correspond to 175° and 355°. If the initial clock of the nanomagnet is pointing right (φ = 0 or 360°), after the stress is released, the tilted nanomagnet will flip counterclockwise to the side that is at a smaller angle to the long axis, which is the $+y$' direction (85°). This is because the nanomagnet needs to cross the right shape anisotropy barrier of the hard axis (see the purple box shown in **Figure 8(b)**) when turning clockwise to the $-y$' direction (265°), whereas when turning counterclockwise, it is not necessary to cross the barrier. Thus the nanomagnet will flip counterclockwise to the $+y$' direction, yielding logic "1." **Figure 8(c)** gives the OOMMF simulations of the preferred magnetization of the nanomagnet with initial clock pointing left or right. As shown in the inset, if the initial state is pointing left, the tilted nanomagnet will rotate counterclockwise to logic "0," whereas if the initial state is pointing right, it will rotate counterclockwise to logic "1."

Based on the preferred magnetization of tilted nanomagnet, a design of dual-input AND/OR magnetic logic gates is proposed, as shown in **Figure 9**. This design is composed of two input nanomagnets A and B, as well as one output tilted nanomagnet Out (clinched 5° clockwise), interacting via ferromagnetic coupling. The magnetization direction of the magnet Out is influenced by the ferromagnetic coupling of the input magnets A and B as well as its own preferred magnetization. As shown in **Figure 9(a)**, if the initial state is pointing left, the nanomagnet Out tends to flip to logic "0." As a consequence, when the inputs A and B are "01," "00," or "10," the output magnet rotates counterclockwise to logic "0," whereas when the inputs A and B are both "1," the output magnet rotates clockwise to logic "1," thereby yielding AND logic. If the initial state is pointing right, as shown in **Figure 9(b)**, the nanomagnet Out tends to flip to logic "1," so when the input magnets A and B are "01," "11," or "10," the output magnet rotates

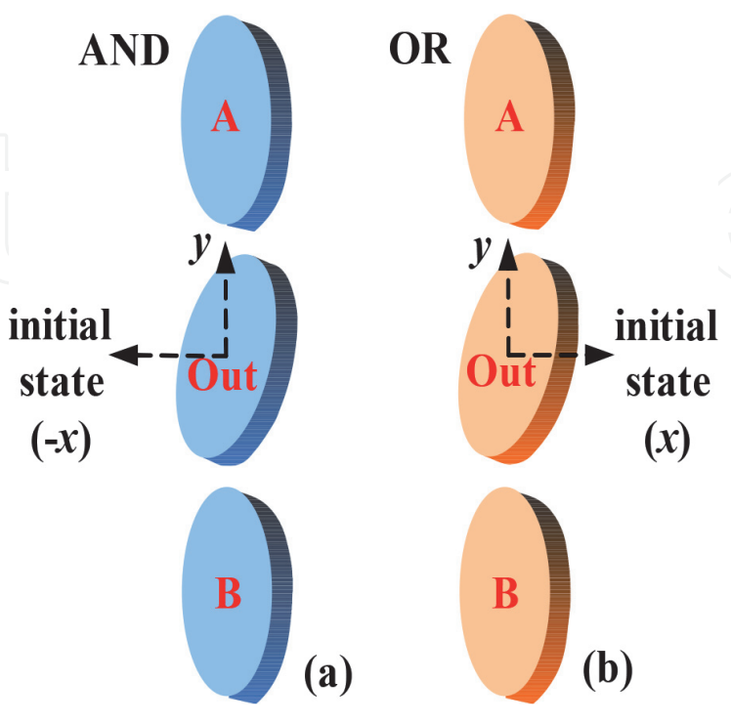

Figure 9.
(a) and (b) show the design of (A) AND logic gate and (B) OR logic gate based on tilted nanomagnet. The initial magnetization of magnet Out is pointing left in (a) and right in (b).

counterclockwise to logic "1," whereas when inputs A and B are both "0," the output magnet rotates clockwise to logic "0," yielding OR logic.

For magnet Out, whose magnetization is interacted by inputs A and B, the dipole–dipole interaction energy writes [7]:

$$E_{\text{dipole}} = \frac{\mu_0 M_s^2 V^2}{4\pi R^3}\left[\begin{pmatrix} -2\cos\varphi_A \sin\theta_A \cos\varphi \sin\theta \\ +\sin\varphi_A \sin\theta_A \sin\varphi \sin\theta + \cos\theta_A \cos\theta \end{pmatrix}\right.$$
$$\left. + \begin{pmatrix} -2\cos\varphi_B \sin\theta_B \cos\varphi \sin\theta \\ +\sin\varphi_B \sin\theta_B \sin\varphi \sin\theta + \cos\theta_B \cos\theta \end{pmatrix}\right] \tag{23}$$

where R is the separation between the centers of neighbor nanomagnets and the magnetization angles of the input magnets are labeled with subscripts A and B.

3.2 Results and discussions

Only OR logic gate is discussed in this section. For shape symmetry, the results will be same for AND logic gate; on account of which, it is not discussed here for clarity. In order to obtain OR logic gate, an initial clock pointing right is necessary. However, whether the clock direction is pointing left or right cannot be controlled simply by the stress. The magnetization vector only tends to be perpendicular to where the stress is applied. Fortunately, for the nanomagnet tilted clockwise by 5°, the direction of initial clock will be determined by the initial magnetization direction of the nanomagnet. As mentioned in Section II, there is no need of crossing the hard axis barrier for the magnet when flipping clockwise. As a consequence, a nanomagnet whose initial state is logic "1" (φ = 90°) tends to flip clockwise under the stress applied in the y direction. It is worth mentioning that if it is not possible to know the initial state of the tilted nanomagnet, a clock pointing right can be obtained by adding a biasing magnetic field pointing right (a stress of 45 MPa and a bias magnetic field of 500 Oe).

The authors assume that the initial state of the nanomagnet Out is logic "1" (φ = 90°, θ = 90°). A stress of 90 MPa is applied to nanomagnet Out for 3 ns. As shown in **Figure 10(a)–(d)**, the nanomagnet flips to "NULL" after the stress has been applied for 1.8 ns. Note that the magnetization of "NULL" state here does not exactly correspond to φ = 0. Rigorously, it makes a certain angle (φ = 7°) with the x axis. This is because the stress field component in the $-y$ direction and the field component of shape anisotropy in the $+y$ direction yield a stable equilibrium, so that the magnetization vector of magnet Out is stably deviated from the x axis. If φ < 10°, the field component of shape anisotropy energy in the $+y$ direction is much smaller than the stress field component, thus not affecting calculation result. Inputs "00," "01," "10," and "11" are read in at 2.9 ns. After the stress has been released for 0.9 ns (t = 3.9 ns), magnet Out will flip to a stable logic state. When the inputs are "01," "10," and "11," magnet Out is logic "1" (φ = 88°), whereas when the inputs are "00," the magnet Out is logic "0" (φ = −92°), successfully yielding OR logic. Note that the nanomagnet Out does not flip to the long axis (φ = 85° or φ = −95°) under the interaction of the ferromagnetic coupling of the input nanomagnets.

The input nanomagnets A and B only produce small fluctuations (∼2°) in the plane and eventually return to the original logic state (φ = 90° or φ = −90°) under the interaction of the ferromagnetic coupling of nanomagnet Out. The angular variations of θ are similar in the four situations. Situation of inputs "10" is specially shown in **Figure 10(e)** and **(f)**. The polar angles (out-of-plane) of initial and final states of the three magnets are all θ = 90°. Magnets A and B produce smaller fluctuations (∼2°) than magnet Out (∼33°), as shown in **Figure 10(e)**.

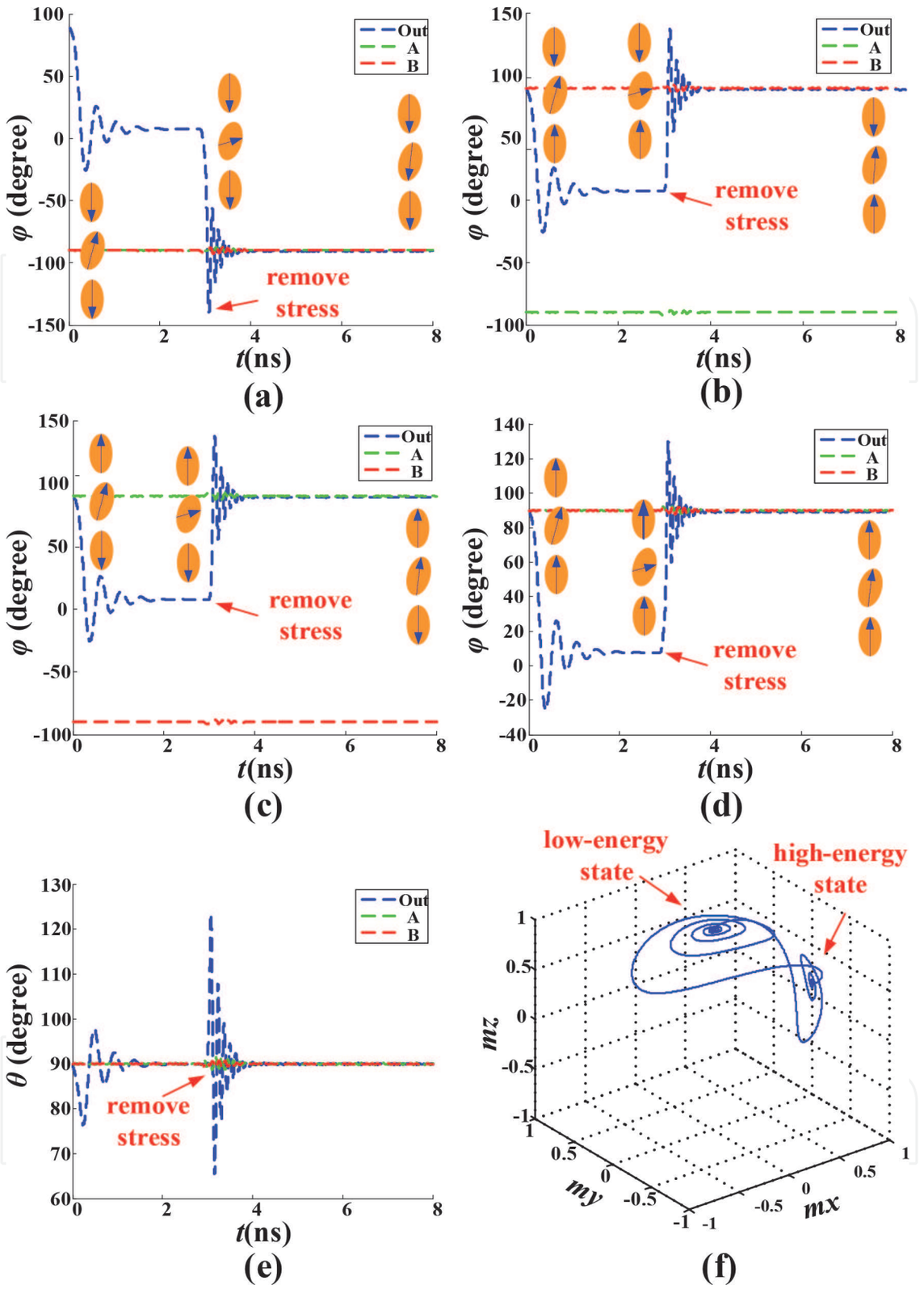

Figure 10.
Apply a stress of 90 MPa to magnet out for 3 ns. (a)–(d) show dynamic magnetization of the azimuth angle φ of (a) input "00," output "0"; (b) input "01," output "0"; (c) input "10," output "0"; and (d) input "11," output "1." when the input is "10," (e) and (f) show (e) dynamic magnetization of the polar angle θ and (f) magnetization track of the nanomagnet out.

The results confirm that magnets A and B will remain stable during the switching of magnet Out. The magnetization track of the magnet Out presents two obvious energy states, as can be seen from **Figure 10(f)**.

Figure 11 shows the simulation of our design of OR logic gate calculated by OOMMF using the data in **Table 1**. The other parameters are set as follows: space size = 800 nm × 200 nm × 20 nm, and mesh size = 5 nm × 5 nm × 5 nm.

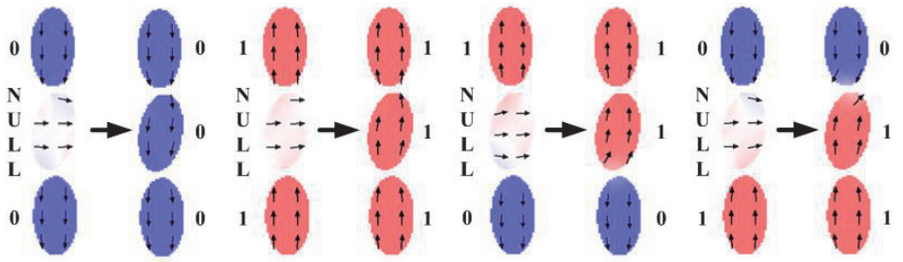

Figure 11.
Simulation results of OR logic gate by OOMMF.

The initial clock is pointing right and the inputs are "10," "01," "00," and "11." Only when the inputs are "00," the output becomes "0"; otherwise the output is "1," yielding OR logic as expected.

Unlike designs based on slanted nanomagnet, basic logic gates based on tilted nanomagnet have three advantages: (1) This tilted magnet design allows high aspect ratio (2:1) nanomagnets to be used; as a consequence of which, less C-shaped and eddy current clock errors will occur; (2) regular-shaped tilted nanomagnet reduces the requirements of fabrication process; and (3) the regular shape provides great convenience in numerical calculation.

3.3 Conclusion

In this section, a design of AND/OR logic gates is proposed based on tilted placement of nanomagnet. The mathematical model of the design is established, and the correctness is verified by the OOMMF software. This scheme can provide a more efficient and reliable basic logic unit for NML design. However, in the experimental preparation, there may be fabrication errors in tilting the placement of the nanomagnet. To reduce the process fabrication error, stress electrodes may be tilted so that the stress will also make an angle with the long axis of the nanomagnet.

4. Conclusions

In this chapter, the multiferroic heterojunction is introduced into the field of spintronics. By utilizing the inverse piezoelectric effect and the inverse magnetostrictive effect in the multiferroic heterojunction, the weak electric field can be used to accurately synchronize the storage and processing of the magnetic logic signal of the uniaxial nanomagnet. Multiferroic nanomagnets are considered to be a strong competitor for post-CMOS devices due to their natural nonvolatility, high radiation resistance, and ultra-low power consumption. In this chapter, the multiferroic nanomagnet device is taken as the research object, and the research on the two key problems of fast nanomagnet rapid reversal magnetization reversal and nanomagnetic logic gate is carried out. The research results have great innovation and application background.

Acknowledgements

This work was supported in part by the National Natural Science Foundation of China (Grant Nos. 61832007) and the National Key R&D Program of China (Grant No. 2018YFB1003304).

DOI: http://dx.doi.org/10.5772/intechopen.91231

Author details

Jiahao Liu* and Liang Fang*
Institute for Quantum Information, State Key Laboratory of High Performance Computing, College of Computer, National University of Defense Technology, Changsha, China

*Address all correspondence to: rae20121220@163.com and lfang@nudt.edu.cn

References

[1] Ma J, Hu J, Li Z, et al. Recent progress in multiferroic magnetoelectric composites: From bulk to thin films. Advanced Materials. 2011;**42**(18): 1061-1087. DOI: 10.1002/adma.201190024

[2] Imre A, Csaba G, Ji L, et al. Majority logic gate for magnetic quantum-dot cellular automata. Science. 2006; **311**(5758):205-208. DOI: 10.1126/science.1120506

[3] Lee J, Dong IS, Park W. The universal magnetic tunnel junction logic gates representing 16 binary boolean logic operations. Journal of Applied Physics. 2015;**117**(17):17D717. DOI: 10.1063/1.4916806

[4] Liu JH, Yang XK, Cui HQ, et al. Modeling of 180° magnetization switching and clock sensitivity in a tilted multiferroic nanomagnet. Journal of Magnetism and Magnetic Materials. 2019;**474**:161. DOI: 10.1016/j.jmmm.2018.10.114

[5] Fidler J, Schrefl T. Micromagnetic modelling-the current state of the art. Journal of Physics D: Applied Physics. 2000;**33**:R135-R156. DOI: 10.1088/0022-3727/33/15/201

[6] Liu JH, Yang XK, Zhang ML, et al. Efficient dipole coupled nanomagnetic logic in stress induced elliptical nanomagnet array. IEEE Electron Device Letters. 2019;**40**(2):220-223. DOI: 10.1109/LED.2018.2889707

[7] Chikazumi S, Charap S. Physics of Magnetism. New York: Wiley; 1964

[8] Fashami MS, Roy K, Atulasimha J, et al. Erratum: Magnetization dynamics, Bennett clocking and associated energy dissipation in multiferroic logic. Nanotechnology. 2011;**22**:155201. DOI: 10.1088/0957-4484/22/30/309501

[9] Brown WF. Thermal fluctuations of a single-domain particle. Physics Review. 1963;**130**:1319-1320. DOI: 10.1103/PhysRev.130.1677

[10] Biswas AK, Bandyopadhyay S, Atulasimha J. Complete magnetization reversal in a magnetostrictive nanomagnet with voltage-generated stress: A reliable energy-efficient non-volatile magneto-elastic memory. Applied Physics Letters. 2014;**105**(7): 072408. DOI: 10.1063/1.4893617

[11] Biswas AK, Ahmad H, Atulasimha J, et al. Experimental demonstration of complete 180° reversal of magnetization in isolated co nanomagnets on a pmn-pt substrate with voltage generated strain. Nano Letters. 2016;**17**(6):3478. DOI: 10.1021/acs.nanolett.7b00439

[12] Roy K, Bandyopadhyay S, Atulasimha J. Binary switching in a symmetric potential landscape. Scientific Reports. 2013;**3**:3038. DOI: 10.1038/srep03038

[13] Zhu W, Xiao D, Liu Y, et al. Picosecond electric field pulse induced coherent magnetic switching in mgo/fept/pt(001)-based tunnel junctions: A multiscale study. Scientific Reports. 2014;**4**(7):4117. DOI: 10.1038/srep041171

[14] Barangi M, Mazumder P. Straintronics: A leap toward ultimate energy efficiency of magnetic random access memories. IEEE Nanotechnology Magzine. 2015;**9**(3):15-24. DOI: 10.1109/MNANO.2015.2441106

[15] Li X, Carka D, Liang C, et al. Strain-mediated 180° perpendicular magnetization switching of a single domain multiferroic structure. Journal of Applied Physics. 2015;**118**(1): 232905-232943. DOI: 10.1063/1.4923350

[16] Peng RC, Hu JM, Momeni K, et al. Fast 180° magnetization switching in a strain-mediated multiferroic heterostructure driven by a voltage. Scientific Reports. 2016;**6**:27561. DOI: 10.1038/srep27561

[17] Jin TL, Hao L, Cao JW, et al. Electric field control of anisotropy and magnetization switching in CoFe and CoNi thin films for magnetoelectric memory devices. Applied Physics Express. 2014;**7**:043002. DOI: 10.7567/APEX.7.043002

[18] Quintero SMM, Martelli C, Braga AMB, et al. Magnetic field measurements based on terfenol coated photonic crystal fibers. Sensors. 2011; **11**(12):11103-11111. DOI: 10.3390/s111211103

[19] Roy K, Bandyopadhyay S, Atulasimha J. Switching dynamics of a magnetostrictive single-domain nanomagnet subjected to stress. Physics Review B. 2011;**83**:224412. DOI: 10.1103/PhysRevB.83.224412

[20] Donahue MJ, Porter DG. 1999. OOMMF User's Guide, Version 1.0. Interagency Report, NISTIR 6367. Available from: http://www.math.nist.gov/oommf

[21] AI-Rashid MM, Bandyopadhyay S, Atulasimha J. Dynamic error in strain-induced magnetization reversal of nanomagnets due to incoherent switching and formation of metastable states: A size-dependent study. IEEE Transactions on Electron Devices. 2016; **63**(8):3307-3313. DOI: 10.1109/TED.2016.2582142

[22] Liu JH, Yang XK, Cui HQ, et al. Voltage pulse-induced fast and repeated switching in a uniaxial nanomagnet at room temperature. Journal of Magnetism and Magnetic Materials. 2019;**491**:165607. DOI: 10.1016/j.jmmm.2019.165607

[23] Gypens P, Leliaert J, Waeyenberge B. Balanced magnetic logic gates in a kagome spin ice. Physics Review Applied B. 2018;**9**:034004. DOI: 10.1103/PhysRevApplied.9.034004

[24] Roy K. Ultra-low-energy non-volatile straintronic computing using single multiferroic composites. Applied Physics Letters. 2013;**103**:173110. DOI: 10.1063/1.4826688